Analysis and Implementation of PS-PWAM Technique for Quasi Z-Source Multilevel Inverter

R.Seyezhai* and D.Umarani[†]

Abstract – Quasi Z-Source Multilevel Inverter (QZMLI) topology has attracted grid connected Photovoltaic (PV) systems in recent days. So there is a remarkable research thrust in switching techniques and control strategies of QZMLI. This paper presents the mathematical analysis of Phase shift- Pulse Width Amplitude Modulation (PS-PWAM) for QZMLI and emphasizes on the advantages of the technique. The proposed technique uses the maximum and minimum envelopes of the reference waves for generation of pulses and proportion of it to generate shoot-through pulses. Hence, it results in maximum utilization of input voltage, lesser switching loss, reduced Total Harmonic Distortion (THD) of the output voltage, reduced inductor current ripple and capacitor voltage ripple. Due to these qualities, the QZMLI with PS-PWAM emerges to be the best suitable for PV based grid connected applications compared to Phase shift-Pulse Width Modulation (PS-PWM). The detailed math analysis of the proposed technique has been disclosed. Simulation has been performed for the proposed technique using MATLAB/Simulink. A prototype has been built to validate the results for which the pulses were generated using FPGA /SPARTAN 3E.

Keywords: Impedance network, Photovoltaic systems, Pulse width amplitude modulation, Quasi Z-source inverter, Shoot-through

1. Introduction

Multilevel inverters (MLI) are evolving as suitable alternative solution for high-power and medium-voltage applications. Especially, the cascaded H-bridge MLI, a transformerless configuration, is gaining tremendous attention in the renewable energy power generation systems [1, 2]. But, the conventional voltage source inverter act only in buck mode which restricts its suitability to PV applications. To extend its application to renewable energy systems, a DC-DC boost converter is required between PV source and H-bridge of the inverter. This two stage conversion from DC to AC requires additional switches and separate control strategies [3, 4]. This finally ends up with reduced efficiency. Also, the conduction of the switches in the same leg leads to short circuit of the source. The output voltage is always lesser than the applied input voltage. Thus, an impedance network comprising of inductors (L) and capacitors (C) are inserted in the front stage of the inverter instead of the DC-DC converter. The resulting topology is called Z-source inverter [5-7]. There are various impedance network configurations of which quasi impedance network is chosen as it has continuous source current from PV, reduced inductor and capacitor

size compared to Z-Source inverter and reduced voltage across one of the impedance network capacitors [8, 9]. Compared to the conventional inverter, QZSI has various advantages. It cuts down the DC-DC converter stage and boosts as well as inverts the input voltage in a single power conversion stage [10-12].

For high power applications, series connection of H-bridges of the inverters form the cascaded H-bridge Multilevel Inverters (CH-MLI).It has high reliability due to its modularity. Higher voltage levels and improved power quality of the output voltage are achieved compared to a conventional inverter. The circuit topology and the modulation strategy remain the same for each module [13-15]. Therefore, this configuration is highly suitable for isolated DC source i.e. PV and fuel cells. A number of such single-phase QZSI can be cascaded to form cascaded H-bridge quasi Z-source multilevel inverter (QZMLI) [16, 17]. The output voltage can be increased to the required level by increasing the number of levels. The cascaded QZSI inherits the advantages of both QZSI and cascaded H-bridge MLI such as improved power quality, reduced number of converter stages and boosted output voltage [18]. The switches of this QZMLI can be controlled by various modulation strategies such as carrier disposition methods and phase shifted PWM. With the conventional PWM strategies, shoot-through controls such as simple boost, maximum boost and maximum constant boost pulses should be added [20, 21]. Shoot-through is a train of pulses that can be added to PWM pulses in order to allow conduction of switches that belongs to the same leg.

[†] Corresponding Author: Renewable Energy Conversion Lab, Department of Electrical and Electronics Engineering, SSN College of Engineering, Kalavakkam, Chennai, India. (umaranid@ssn.edu.in)

* Renewable Energy Conversion Lab, Department of Electrical and Electronics Engineering, SSN College of Engineering, Kalavakkam, Chennai, India. (seyezhair@ssn.edu.in)

Generally, for any MLI, the phase shift PWM is applied. Even if it has balanced switching action, it suffers from disadvantages such as higher switching loss, reduced fundamental and efficiency [22, 23]. To mitigate the aforementioned disadvantages, phase shifted pulse width amplitude modulation (PS-PWAM) technique has been proposed for QZMLI. A detailed mathematical analysis, pulse generation logic, design of impedance network and comparison of various parameters with conventional PWM technique have been elaborated. Simulation has been carried out for the proposed technique and the results are validated with hardware prototype.

Section II illustrates the working principle and operating states of five-level QZSI. In section III, PWAM strategy has been clearly discussed. A complete review of pulse generation logic, mathematical analysis, gating pattern and design has been provided. The simulation results of the proposed technique and hardware prototype has been disclosed in section IV and V respectively. In the final section, the work is concluded and references are provided.

2. Quasi Z-Source Multilevel Inverter

Quasi Z-source inverter falls under the category of impedance (Z) source inverters. It has various derivatives and suitable for high and medium power applications. The peculiar L and C network (Impedance network) that is introduced to the inverter paves the way for its various advantages [25-27].

- It can operate as buck / boost inverter. PV based applications are generally operated in boost mode.
- There is no need of dead time between switching of the devices as the conduction of devices in the same leg doesn't allow short circuit of the DC/PV source.
- It can operate in shoot-through state by converting some of the zero states to shoot-through states. During this period the input voltage is boosted by the impedance network.
- It draws continuous input current from the PV source that is required for PV applications.
- The size of the impedance network is reduced compared to the conventional Z-source inverter.

Fig. 1 shows the circuit diagram of single-phase five-level QZSI. Two H-bridges QZSI can be cascaded to form a five level QZSI. Each of these bridges work like a standard QZSI and has two operating states such as shoot-through and non-shoot through state. During the nonshoot-through state, the power is delivered to the load like a traditional H-bridge inverter (HBI). During the shoot-through state, the impedance network involves in boosting the input voltage, and power is not transferred to the load. Since five level QZSI is a hybrid of conventional HBI and QZSI, the output of MLI is given by,
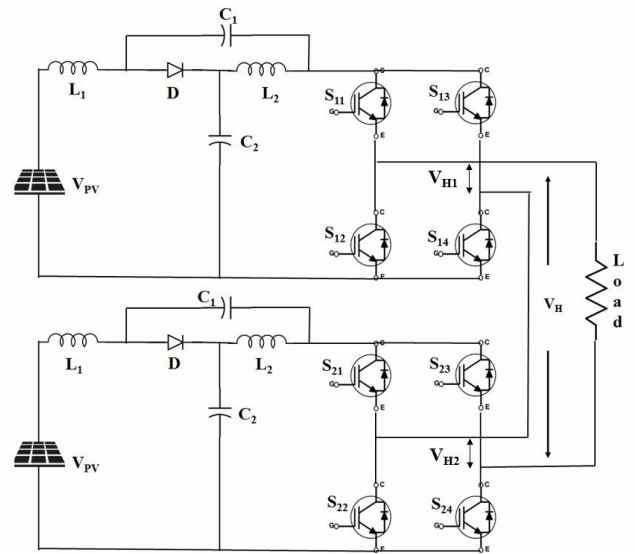

Fig.1. Five level QZSI

$$V_H = V_{H1} + V_{H2} \tag{1}$$

Where, V_H is the cascaded multilevel output voltage, V_{H1} and V_{H2} are the output voltages of individual H-bridges.

$$V_{DC} = V_{C1} + V_{C2} \tag{2}$$

$$V_{DC} = \frac{1}{1-2D} V_{PV} \tag{3}$$

$$V_{C1} = \frac{1-D}{1-2D} V_{PV} \tag{4}$$

$$V_{C2} = \frac{D}{1-2D} V_{PV} \tag{5}$$

Where, V_{DC} is the DC link voltage of the QZSI, V_{PV} is the PV panel voltage to each H-bridge QZSI , V_{C1} and V_{C2} are the capacitor voltages of the impedance network, and D is the shoot-through duty ratio.

2.1 Design of QZSI network

A single phase AC system is always associated with second harmonic ripple. So, based on the 2ω ripple analysis of the single phase QZSI, the impedance network has been designed [28-30]. The 2ω power $P_{o-2\omega}$ is completely stored in capacitors and the

$$\text{QZS Capacitance is } \quad C = \frac{2V_o I_o}{\omega \varepsilon V_{PN}^2} \tag{6}$$

Where, V_O is the output voltage, I_O is the output current, V_{PM} is the DC link voltage, and ε is the engineering tolerance for capacitor taken as 5%.

To limit the switching frequency ripple, the QZS inductance is

Table 1. Design parameters

Design parameter	Value
Switching frequency , f_s	10kHz
Modulation index , M	0.8
Input voltage , V_{DC}	5V
DC link voltage	8.5V
Boost factor	1.66

$$L = \frac{D(1-D)T_S V_{DC}}{2(1-2D)\Delta i} \qquad (7)$$

Where, Δi is the switching ripple of inductor current, D is the shoot-through duty ratio, T_S is the switching time period and V_{DC} is the input DC voltage.

Based on the Eqs. (6) and (7), the inductance and capacitance values are calculated as 3mH and 2200μF respectively. Table 1 shows the design parameters.

3. Pulse Width Amplitude Modulation

The operation of an inverter requires proper switching of the devices. Modulation of multilevel inverters is a challenging research where carrier based pulse width modulation technique forms a common thread. Yet every topology will be working on specific PWM strategy. There are various carrier displacement and carrier shift methods for generating pulses. Among the two, the carrier phase shift technique consists of specific advantages. The carrier displacement method is classified into phase disposition, phase opposition disposition and alternate phase opposition disposition. For QZSI, modifications are done in the pulse pattern by including additional shoot through states. This gives rise to three important modulation strategy namely simple boost, maximum boost and maximum constant boost PWM techniques. These strategies differ by the magnitude of the shoot through line [31, 32]. Each switching cycle has a shoot through period T_S and a non-shoot through period T_O. With T as the time period,

$$T = T_S + T_O \qquad (8)$$

$$D_S = \frac{T_S}{T} \qquad (9)$$

$$D_O = \frac{T_O}{T} \qquad (10)$$

Hence, $D = D_O + D_S = 1$

D_S is the shoot through duty ratio and D_O is the non-shoot through duty ratio

For the cascaded multilevel inverter, phase-shifted carrier pulse width modulation (PS-PWM) is the commonly applied strategy and the THD reduction is achieved. The sinusoidal reference waveforms of the right leg and left leg of the two H-bridges are shifted by 180° and each triangular carrier is phase shifted by 180°/N (N-Number of bridges). This
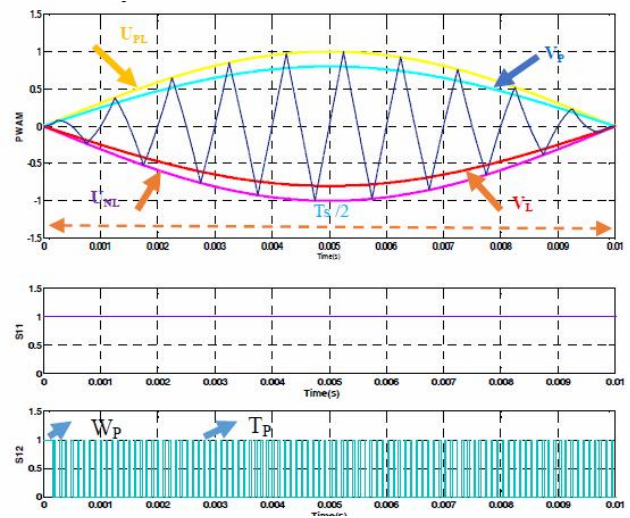
Fig. 2. PWAM with shoot-through and PWM

modulation strategy results in the cancellation of associated sideband harmonics upto the Nth carrier group. The conventional phase shifted PWM has balanced switching action yet it has higher switching loss. Therefore, the proposed PS-PWAM utilizes the balanced switching action from the phase shifted carrier and reduces switching loss by pulse amplitude modulation. It has higher voltage utilization than the traditional PS-PWM technique [33, 34]. The detailed pulse generation logic of PS-PWAM is explained as follows:

3.1 Pulse generation logic

Fig. 2 represents the pulse width amplitude modulation technique applied to the five level QZSI. The modulation waves of the left bridge legs is U_{PL} while the modulation waves of right bridge legs is U_{PR}. The carrier wave is shown as $A\{1,2\}$. The switching pattern of the single bridge is shown as $S_1\{1,2,3,4\}$. The top and bottom shoot-through envelopes are shown as $ST\{P, N\}$. The amplitude of the carrier varies between top and bottom envelopes of the modulation waves. They are represented by

$$Y_{max} = \max\ \{U_{PL}, U_{PR}\} \qquad (11)$$

$$Y_{min} = \min\ \{U_{PL}, U_{PR}\} \qquad (12)$$

In this PWAM, shoot-through is added by maximum boost control. The shoot-through reference can be obtained by multiplying a λ factor with top and bottom envelopes of modulation waves. i.e. λY_{max} and λY_{min} . The value of λ can be changed between 0.5 to 1 p.u. The shoot-through duty ratio of PWAM is given by

$$D_{PWAM} = \frac{T_{sh}}{T} = 1 - \lambda \qquad (13)$$

The modulation scheme can be described in easy steps

for one H-bridge of the five level QZSI, and same logic can be extended for the second H-bridge with phase shifted carrier.

- For left leg of the H-bridge,
1. The upper switch S_{11} turns on all the time without switching action when the modulation wave is maximum in $U\{P,N\}L$.
2. The lower switch, S_{12} switches only when the carrier is greater than the top envelope V_P or lower than bottom envelope V_N.
3. The lower switch S_{12} switches on all the time without switching action when the modulation wave is minimum in $U\{P, N\}L$.
4. The upper switch, S_{11} switches only when the carrier is greater than the top envelope V_P or lower than bottom envelope V_N.
- For right leg of the H-bridge,
  The modulation strategy remains the same as that of left-bridge legs, but the modulation waves $U\{P,N\}R$ possesses a phase difference of 180°.
- The stepped voltage waveform can be synthesized by employing a phase difference of 90° between adjacent carriers.

3.2 Mathematical Analysis of PS-PWAM

The pulse width amplitude modulation technique implemented in the proposed inverter is clearly analyzed to identify the state of the pulses, the way they are generated and how the shoot-through states are included in the final pulse.

The frequency f_r of reference signal sets the output frequency f_o and the frequency f_s of carrier signal sets the number of pulses per half cycle (m).

$$M = \frac{V_r}{V_C} \tag{14}$$

Where, V_r is the amplitude of the reference signal, and V_c is the amplitude of carrier signal.

$$M_f = \frac{f_c}{f_r} \tag{15}$$

Where, f_c is the carrier frequency, and f_r is the reference frequency in Hz.

To calculate the pulse width W_P:

Let α_P be the angle of intersection of reference and carrier signal.

It is know that $\alpha = \omega * t$

$$\therefore t = \frac{\alpha}{\omega}, \omega = 2\pi f \tag{16}$$

It is assumed that the positive pulses start at $\omega_P t_P = \alpha_P$

$$\therefore t_P = \frac{\alpha_P}{\omega_P} \text{ or } t_P = \frac{\alpha_P + \pi}{\omega_P} \tag{17}$$

where, P is the pulse number.

Let T_S be the switching cycle considered. For sinusoidal pulse width modulation,

$$t_P = t_x + \frac{PT_s}{2}, \quad P = 1, 2, 3, \dots m \tag{18}$$

where, m is the number of pulses per half cycle .

For odd pulses,

$$1 - \frac{2T}{T_S} = M \sin[\omega(t_x + \frac{PT_S}{2})]; P = 1, 3, 5 \dots, 2m \tag{19}$$

For even pulses,

$$\frac{2T}{T_S} = M \sin[\omega(t_x + \frac{PT_S}{2})], P = 2, 4, 6 \dots 2m \tag{20}$$

where, M is the modulation index.

$$T_S = \frac{T}{2(m+1)} \tag{21}$$

Solving Eqs. (17) and (18) results in,

$$2M \sin[\omega(t_x + \frac{PT_S}{2})] = 1 \tag{22}$$

$$\therefore t_x = \frac{1}{\omega} \sin^{-1}(\frac{1}{2M}) - \frac{PT_S}{2} \tag{23}$$

Time instant of the PWM pulse,

$$\begin{aligned} t_P = t_x + \frac{PT_S}{2} &= \frac{1}{\omega} \sin^{-1}(\frac{1}{2M}) - \frac{PT_S}{2} + \frac{PT_S}{2} \\ &= \frac{1}{\omega} \sin^{-1}(\frac{1}{2M}) \end{aligned} \tag{24}$$

Width of the pulse,

$$W_P = t_{P+1} - t_P = \frac{\alpha_{P+1}}{\omega} - \frac{\alpha_P}{\omega} = \frac{\delta_P}{\omega} \tag{25}$$

where, δ_P is the pulse angle of Pth pulse.

For shoot-through, the pulses are generated similar to maximum boost control. So, the duty ratio is kept constant.

For modulation index M, the maximum active state duty ratio is $D_{A\max}$.

$$D_{A\max} = \max \left[\frac{M \sin \omega t - M \sin(\omega t - \frac{2\pi}{3})}{2} \right] \tag{26}$$

At 60°,

$$D_{A\max} = \left[\frac{M\sin 60° - M\sin(60° - 120°)}{2}\right] \quad (27)$$

$$= \frac{2M\sin 60°}{2} = M\frac{\sqrt{3}}{2}$$

The maximum shoot-through duty ratio that can be obtained is $D_{O\max}$.

$$D_{O\max} = 1 - D_{A\max} = 1 - \frac{\sqrt{3}}{2}M \quad (28)$$

The longest shoot-through period that can be calculated is $T_{O\max} = T_S(D_{O\max} - D_{O\min})$

$$T_{O\max} = T_S\left(\left(1 - \frac{\sqrt{3}M}{2}\right) - \left(\frac{1-M}{2}\right)\right) = \frac{T_S}{2}\left[1 + M(1 - \sqrt{3})\right] \quad (29)$$

Let, $T_{O\max} = T_P$ be the width of the shoot through pulse. For each shoot-through pulse, the width remains the same. The pulse width W_P is merged with the shoot-through pulse width T_P using logical OR operation.

If $W_P > T_P$ or (T_P lies within W_P) then W_P will be the width of the resulting pulse. If PWAM operates in zero state, T_P will be the width of the pulse.

Let T is the output pulse state and given by,

$$T = \alpha W_P(t) + (1-\alpha)T_P(t) \quad (30)$$

Let $V_{TP}(t)$ is the state of $T_P(t)$, $V_{WP}(t)$ is the state of $W_P(t)$ and $V_T(t)$ is the state of $T(t)$.

$$\therefore V_T(t) = \alpha V_{WP}(t) + (1-\alpha)V_{TP}(t) \quad (31)$$

There arises four case studies based on high and low state of the PWAM pulse and shoot-through pulse for $t(0:0.02)$ second. The cases are listed in Table 2.

Table 2. Cases for PWAM

Case	α	V_{WP}	V_{TP}	V_T
Case I	0	L	L	V_{TP}
Case II	0	L	H	V_{TP}
Case III	1	H	L	V_{WP}
Case IV	0.5	H	H	1

From the four cases, it can be inferred that the output pulse of the PS-PWAM technique is obtained only when one of the two states of PWM V_{WP} or Shoot-through V_{TP} is high. It is exactly like an OR operation of the PWM pulse and shoot-through pulse.

3.3 Gating pattern

Based on the above four cases, the pulses are generated
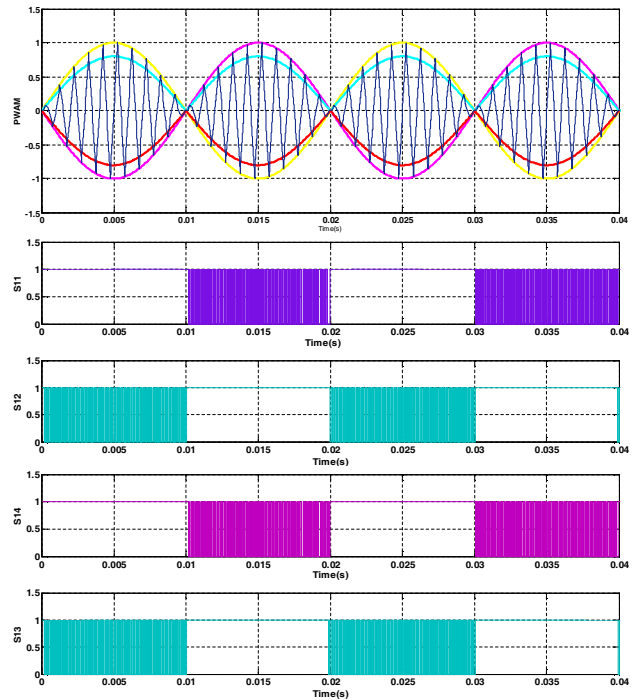
Fig. 3. Gating Pattern of PS-PWAM technique

Table 3. Simulation parameters

Design Parameter	Value
Switching frequency , f_s	10kHz
Input Voltage , V_{DC}	5V
DC link Voltage	8.5V
Inductance L_1 and L_2	3mH
Capacitors C_1 and C_2	2.2mF
Load Resistor	100Ω
Boost factor	1.66
Filter Inductor	25mH
Filter capacitor	100µF

and the gating pattern of the proposed technique is presented in Fig. 3. The modulating signal and the triangular carrier is shown for two fundamental cycles. The pulses of S_{11}, S_{12}, S_{13} and S_{14} of the first H-bridge is depicted clearly.

3.4 Simulation results

The simulation circuit of single-phase five level QZSI was modelled using MATLAB/Simulink to analyze the proposed PWAM strategy. The simulation parameters are listed in Table 3. The MATLAB/Simulink model and the output voltage is shown in Fig. 4 (a) and (b).

3.5 Performance Analysis – PS-PWM & PS-PWAM

The performance parameters of the PS-PWM and PS-PWAM technique applied for five level QZSI was studied and compared based on the boost factor, total harmonic distortion of output voltage, inductor current ripple, capacitor voltage ripple and switching losses. The FFT
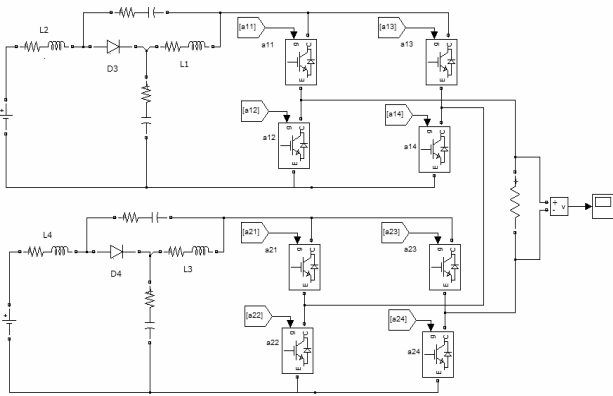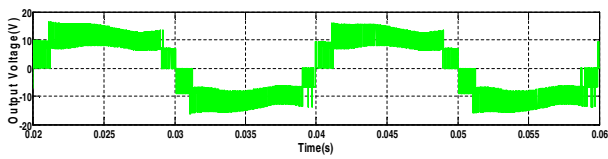
Fig. 4(a). Simulink model of five level QZSI

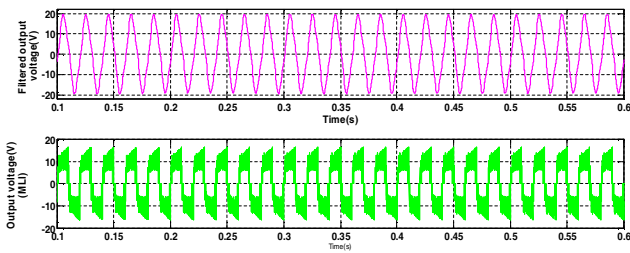**Fig. 4**(b). Output voltage of five level QZSI

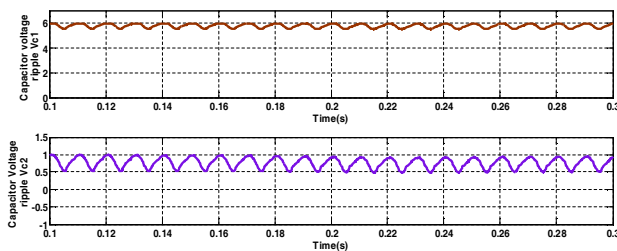**Fig. 5.** Filtered and stepped output voltage of five level QZSI (PS-PWAM)

Fig. 6. Capacitor voltage ripple V_{C1} and V_{C2} of the QZS network (PS-PWAM)

analysis results and the waveforms are discussed in this section. Fig. 5 shows the filtered output voltage and stepped output voltage of MLI. Fig. 6 and Fig. 7 depict the capacitor voltage and inductor current ripple of the QZS network respectively. The THD of output voltage is shown in Fig. 8 for the five level QZSI using PS-PWAM technique.

The PS-PWAM technique applied to the proposed inverter has provided an output voltage of 18.8 V (peak) for an input voltage of 5 V per bridge. By using an LC filter, the output voltage THD has been obtained as 1.09%.
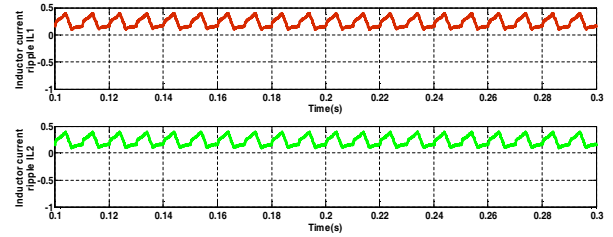

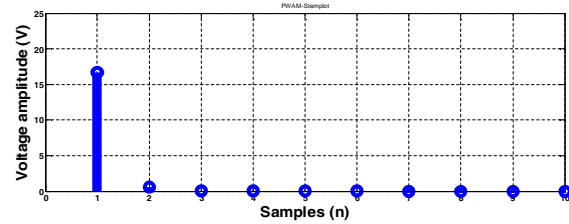**Fig. 7.** Inductor current ripple I_{L1} and I_{L2} of the QZS network (PS-PWAM)

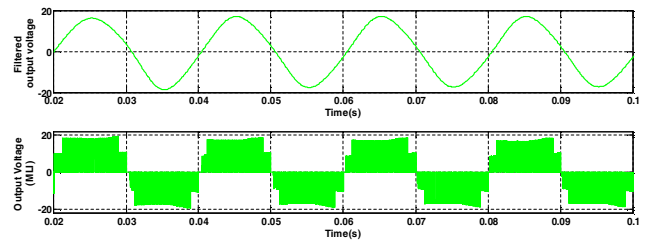**Fig. 8.** FFT analysis of PS_PWAM for five level QZSI

Fig. 9. Filtered and stepped output voltage of five level QZSI using PS-PWM
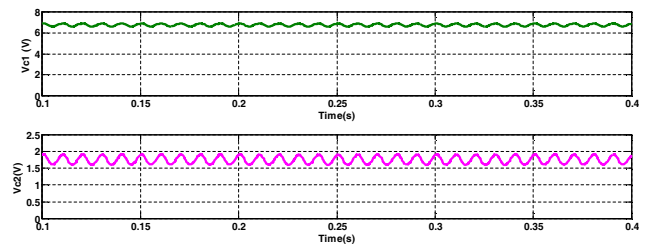

Fig. 10. Capacitor voltage ripple V_{C1} and V_{C2} of the QZS network (PS-PWM)

Fig. 9 shows the filtered output voltage and stepped output voltage of five level QZSI with PS-PWM modulation technique. The capacitor voltage ripple, inductor current ripple and plot of the THD are shown in figures 10, 11 and 12 respectively for the five level QZSI using PS-PWM technique.

The conventional PS-PWM technique applied to the proposed inverter has provided an output voltage of 18.36 V (peak) for an input voltage of 5 V per H-bridge. By using an LC filter, a THD of 3.08 % has been obtained. Table 4 lists the parameters of loss calculation. Table 5 illustrates the comparison of parameters between PS-PWM and PS-PWAM modulation techniques.
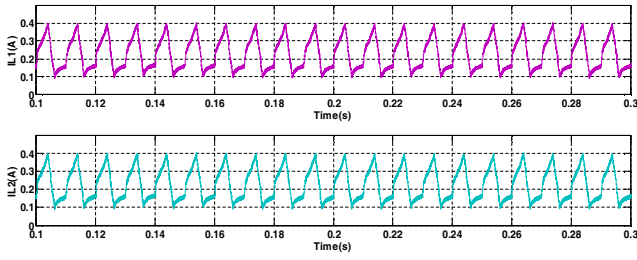
Fig. 11. Inductor current ripple I_{L1} and I_{L2} of the QZS network (PS-PWM)
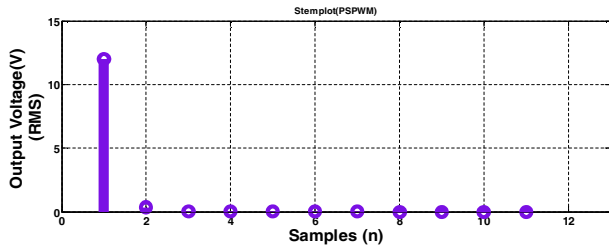

Fig. 12. FFT analysis of PS-PWM for five level QZSI

The switching loss has been calculated by the rise time and fall time of the switch voltage and current during active and shoot-through states.

For PS-PWM, the switching loss is represented by,

$$P^{PS-PWM}{}_{SW(ACT+ST)} = 0.5V_{in}I_o(T_r + T_f)f_{SW} + P_{F,ST}I_L \quad (32)$$

Where, V_{in} is the input voltage, I_o is the output current, T_r is the rise time, T_f is the fall time of the switching, f_{SW} is the switching frequency, $P_{F,ST}$ is the power loss during shoot-though and I_L is the load current.

$$P_{F,ST} = \frac{f_{SW}(E_{ON} + E_{OFF})V_{dc}}{V_{ref}I_{ref}} \quad (33)$$

Where, f_{SW} is the switching frequency; E_{ON} is the turn-on switching loss, E_{OFF} is the turn-off switching loss energy per pulse of each MOSFET IRFP540, V_{dc} is the dc-link voltage, V_{ref} and I_{ref} are the switching voltage and current of the switches.

For PS-PWAM, the switching loss includes the shoot-through loss in the right and left leg of the H-bridge inverter [28]. It is calculated as follows.

$$P^{PS-PWAM}{}_{SW(ACT+ST)} = 13.4\% P^{PS-PWM}{}_{SW} + 50\% P^{PS-PWM}{}_{SW} + P_{F,ST}I_L \quad (34)$$

The conduction loss P_{con} is calculated by

$$P_{con} = I_o{}^2 R_{DS\_ON} \quad (35)$$

Where, I_O is the output current and R_{DS_ON} is the MOSFET on-state resistance.

Table 4. Loss calculation parameters (Simulation)

Parameter	Rating	Parameter	Rating
V_{in}	10 V	E_{OFF}	150μJ
I_{in}	2 A	f_{SW}	10kHz
T_r	52ns	V_{ref}	8.5V
T_f	48ns	I_{ref}	1 A
E_{ON}	105μJ	R_{DS_ON}	0.077Ω

Table 5. Comparison between PS-PWM and PS-PWAM

PARAMETER	PS-PWM	PS-PWAM
Peak output voltage	18.36 V	18.8 V
Output voltage THD with ripple	3.08 %	1.09%
Inductor current ripple	1.4%	1.23%
Capacitor voltage ripple	0.77%	0.698%
Switching loss, P_{SW}	1.216 W	1.087 W
Efficiency, η%	93.92%	94.56%

The efficiency has been calculated by,

$$\eta\% = \frac{P_{in} - (P_{SW} + P_{con})}{P_{in}} * 100 \quad (36)$$

where, $P_{in} = V_{in} * I_{in}$ is the total input power and P_{SW} is the switching loss and P_{con} is the conduction loss.

The conduction and switching loss parameters are listed in Table 4. The values T_r and T_f were measured from the simulation waveform. Using Eqs. (32), (33) and (34) the switching loss for PS-PWM has been calculated as 1.216 W and PS-PWAM as 1.087 W. The conduction loss has been calculated as 0.616 W using Eq. (35).

From Table 5, the PS-PWAM technique proves to be a better modulation technique for QZSI. The switching loss has been reduced and the power quality has been improved compared to PS-PWM [35].

4. Hardware Implementation

A prototype of the single-phase five level QZSI has been built. The proposed PS-PWAM pulses generated using the interface of MATLAB/Xilinx. The pulses have been provided to the switching devices using FPGA-SPARTAN 3E processor. The hardware circuit is shown in Fig. 13 and the design parameters used for the simulation shown in Table 3 have been used for hardware implementation as well. The generated pulse pattern is shown in Fig. 14. Fig. 15 shows the switch voltage and switch current of MOSFET. An input voltage of 5V has been applied to each H-bridge of the five level QZSI. The stepped output voltage waveform and filtered output voltage waveform are shown in Fig. 16(a) and (b) respectively. The output voltage has been boosted to 1.66 times the input voltage as per the design.

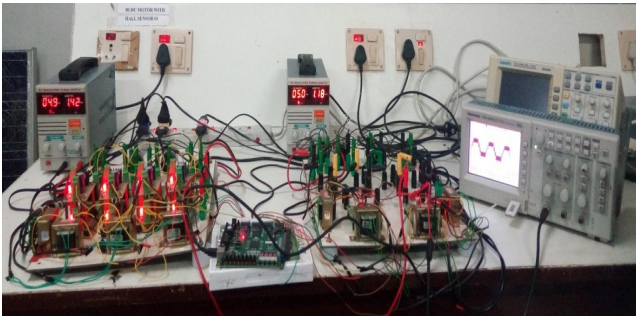The voltage across the MOSFET and the current through
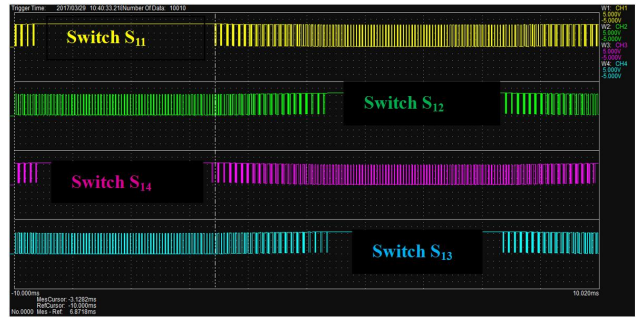
Fig. 13. Hardware prototype of five level QZSI
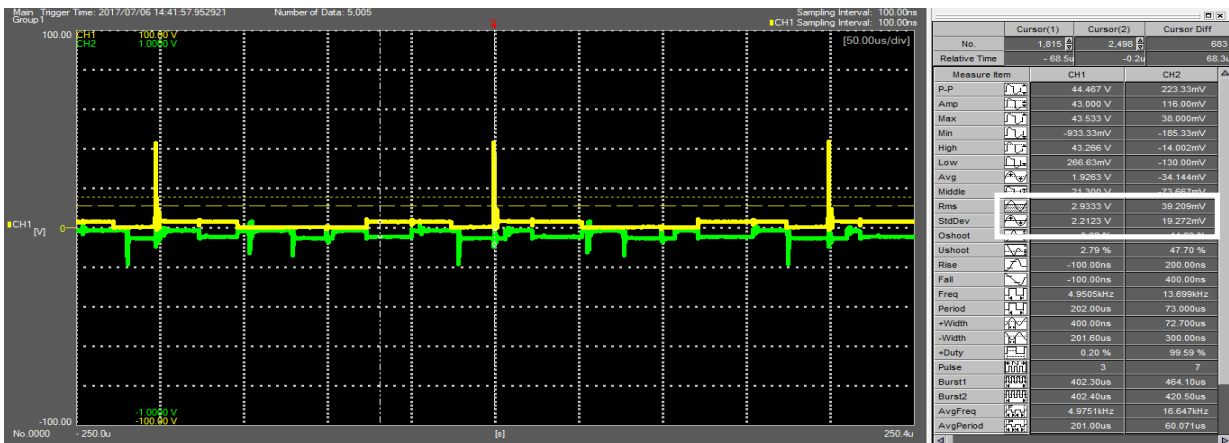

Fig. 14. Gating pattern of the PS-PWAM

Fig. 15. Switch voltage and current of MOSFET IRFP540

Table 6. Loss calculation parameters (Hardware)

Parameter	Rating	Parameter	Rating
V_{in}	10 V	E_{OFF}	150μJ
I_o	1 A	f_{SW}	10kHz
T_r	100ns	V_{ref}	8.5V
T_f	100ns	I_{ref}	1.2 A
E_{ON}	105μJ	P_{con}	0.616 W

Table 7. Comparison of switching loss and efficiency

	Switching loss (W)	Efficiency (%)
PS-PWM (Simulation)	1.216	93.92
PS-PWM (Hardware)	2.216	88.92
PS-PWAM(Simulation)	1.087	94.56
PS-PWAM (Hardware)	1.466	92.67

the MOSFET have been measured using Scopecorder DL850 for calculating the switching loss. The waveform parameters were analyzed with X-Viewer software. Using the measured values and parameters shown in Table 6, the switching loss for PS-PWM is found as 2.216 W and for PS-PWAM is found as 1.466 W.

The comparison of switching loss and efficiency has been presented in Table 7.

An LC filter was designed with L = 100mH and C=100
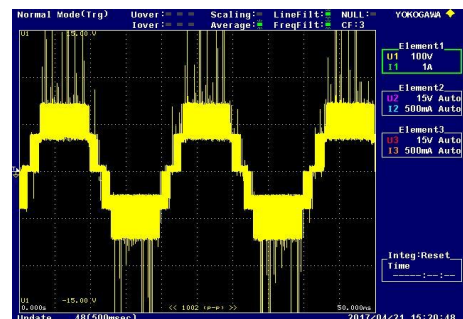

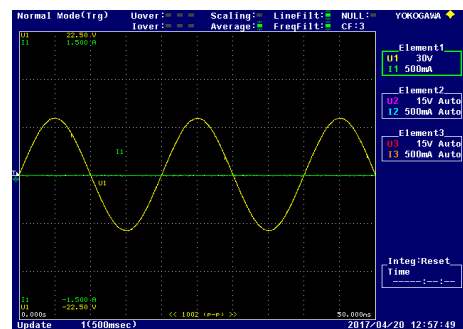**Fig. 16**(a). Five level output voltage of QZSI

Fig. 16(b). Filtered output voltage of five level QZSI

μF. The filtered output voltage of the inverter shown in Fig. 16(b) is 22.5 V which has been boosted from 5 V per H-

Fig. 17. The output voltage THD of five-level QZSI for R Load

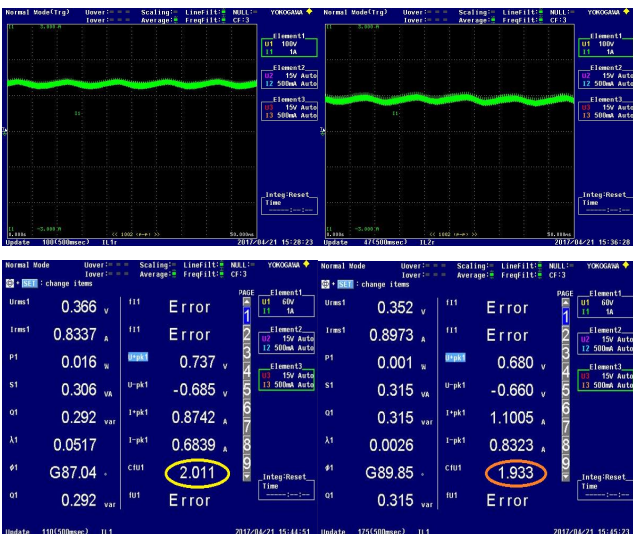**Fig.18.** Capacitor voltage ripple V_{C1} and V_{C2}

Fig. 19. Inductor current ripple I_{L1} and I_{L2}

Table 8. Validation of hardware results

Parameter	PS-PWM	PS-PWAM
Peak output voltage	22.5 V	22.5 V
Output voltage THD with filter	6.645 %	1.131 %
Inductor current ripple	2.85 %	2.01 %
Capacitor voltage ripple	1.36 %	1.14 %
Switching loss, P_{SW}	2.216 W	1.466 W
Efficiency, η%	88.92 %	92.67 %

bridge. The THD of the output voltage has been obtained as 1.131% and is shown in Fig. 17.

The capacitor voltage ripple and inductor current ripple waveforms are shown in Figs. 18 and 19 respectively. The capacitor voltage ripples were found to be 1.14% and 1.09% for V_{C1} and ΔV_{C2}. Similarly, the inductor current ripple values were found to be 2.01% and 1.93% for ΔI_{L1} and ΔI_{L2}.

The hardware results were validated with the simulation results and listed in Table 8. The parameters such as output voltage THD, peak output voltage, inductor current ripple and capacitor voltage ripple were measured using power quality analyzer WT500 and have been found to be better than the conventional PS-PWM technique.

5. Conclusion

In this paper, a detailed mathematical analysis of the phase shift pulse amplitude modulation technique for single phase five level QZSI has been presented. The pulse generation technique has been disclosed highlighting its advantages. The comparison of the proposed technique and the conventional PWM technique was carried out based on parameters such as output voltage THD, peak output voltage, inductor current ripple and capacitor voltage ripple. From the results it can be concluded that the proposed PS-PWAM technique provides reduced output voltage THD of 1.131% compared to 6.645% of PS-PWM technique. The reduced THD results in improved power quality. The inductor current ripple of 2.01% and capacitor voltage ripple of 1.14% are very less compared to the conventional PS-PWM. The switching loss of the PS-PWAM has been reduced by 1.5 times than the PS-PWM technique. The simulation and experimental results are presented to verify the features of the proposed phase shift pulse width amplitude modulation. The PS-PWAM technique proves to be better than the conventional PS-PWM for single-phase five level QZSI.

Acknowledgements

References

[1] Banaei, M. R., and E. Salary. "Asymmetric Cascaded Multi-level Inverter: A solution to obtain high number of voltage levels," *Journal of Electrical Engineering and Technology*, vol. 8, no. 2, pp. 316-325, 2013.

[2] Rodriguez, Jose, Jih-Sheng Lai, and Fang Zheng Peng. "Multilevel inverters: a survey of topologies, controls, and applications," *IEEE Transactions on Industrial Electronics*, vol. 49, no. 4, pp. 724-738, 2002.

[3] Peng F. Z., Yuvan X., Fang X. and Qian Z., "Z-source inverter for motor drives," *IEEE Transactions on Power Electronics*, vol. 20, no. 4, pp. 857-863, 2005.

[4] Y. Huang, M.S. Shen, F.Z. Peng, J. Wang, "Z-Source inverter for residential photovoltaic systems," *IEEE Trans on Power Electron.*, vol. 21, no. 6, pp. 1776-1782, Nov. 2006.

[5] U. Supatti, F.Z. Peng, "Z-source inverter with grid connected for wind power system," *IEEE Energy Conversion Congress and Exposition, ECCE 2009, San Jose, USA*, pp. 398-403, 20-24 Sep. 2010.

[6] Trinh, Quoc-Nam, and Hong-Hee Lee., "A new Z-source inverter topology with high voltage boost ability." *Journal of Electrical Engineering and Technology*, vol. 7, no. 5, pp. 714-723, 2012.

[7] Peng F. Z., "Z-source inverter," *IEEE Transactions on Industrial Applications*, vol. 39, no. 2, pp. 504-510, 2003.

[8] Siwakoti, Yam P., Fang Zheng Peng, Frede Blaabjerg, Poh Chiang Loh, and Graham E. Town. "Impedance-source networks for electric power conversion part I: a topological review," Power Electronics, *IEEE Transactions,* vol. 30, no. 2, pp. 699-716, 2015.

[9] Siwakoti, Yam P., Fang Zheng Peng, Frede Blaabjerg, Poh Chiang Loh, Graham E. Town, and Shuitao Yang. "Impedance-source networks for electric power conversion part II: review of control and modulation techniques," *Power Electronics, IEEE Transactions*, vol. 30, no. 4, pp., 1887-1906, 2015.

[10] Deng, Kai, Fei Mei, Jun Mei, Jianyong Zheng, and Guangxu Fu., "An extended switched-inductor quasi-Z-source inverter," *Journal of Electrical Engineering and Technology*, vol. 9, no. 2, pp. 541-549, 2014.

[11] Anderson, Joel, and Fang Z. Peng. "Four quasi-Z-source inverters," *Power Electronics Specialists Conference, 2008. PESC 2008. IEEE*, pp. 2743-2749. IEEE, 2008.

[12] Jagan, Vadthya, Janardhana Kotturu, and Sharmili Das. "Enhanced-Boost Quasi-Z-Source Inverters with Two Switched Impedance Network." IEEE Transactions on Industrial Electronics 2017.

[13] J.-S. Lai and F. Z. Peng, "Multilevel converters — A new breed of power converters," *IEEE Transactions on Industrial Applications*, vol. 32, pp. 509-517, May/June 1996.

[14] Ajami, Ali, Ataollah Mokhberdoran, and Mohammad Reza Jannati Oskuee. "A new topology of multilevel voltage source inverter to minimize the number of circuit devices and maximize the number of output voltage levels," *J Electr Eng Technol*, vol. 8, no. 6, 1321-1329, 2013.

[15] Gholinezhad, Javad, and Reza Noroozian. "Analysis of cascaded H-bridge multilevel inverter in DTC-SVM induction motor drive for FCEV." *Journal of Electrical Engineering and Technology*, vol. 8, no. 2, pp. 304-315, 2013.

[16] D. Sun, B. Ge, F.Z. Peng, A. Haitham, D. Bi, Y. liu, " A new grid connected PV system based on cascaded H-bridge quasi-Z source inverter," *2012 IEEE International Symposium on Industrial Electronics (ISIE)*, pp. 951-956, 28-31 May, 2012

[17] Yan Zhou, Liming Liu, Hui Li, "A high-performance photovoltaic module-integrated converter (MIC) based on cascaded quasi-Z-source inverters (qZSI) using eGaN FETs," *IEEE Transactions on Power Electronics*, vol. 28, no. 6, pp. 2727-2738, June 2013.

[18] Battiston, Alexandre, El-Hadj Miliani, Serge Pierfederici, and Farid Meibody-Tabar. "A Novel Quasi-Z-Source Inverter Topology with Special Coupled Inductors for Input Current Ripples Cancellation." *IEEE Transactions on Power Electronics*, vol. 31, no. 3, pp. 2409-2416, 2016.

[19] B. P. McGrath and D. G. Holmes, "A comparison of multicarrier PWM strategies for cascaded and neutral point clamped multilevel inverters," *in Proc. IEEE PESC*, 2000, pp. 674-679.

[20] S. Thangaprakash and A. Krishnan, "Implementation and Critical Investigation on Modulation Schemes of Three Phase Impedance Source Inverter," *Iranian Journal of Electrical & Electronic Engineering*, vol. 6, no. 2, June 2010.

[21] Shen M., Wang J., Joseph A. and Peng F. Z., "Constant boost control of the Z-source inverter to minimize current ripple and voltage stress," *IEEE Transactions on Industry Applications*, vol. 42, no. 3, pp. 770-778, June 2006.

[22] Aleenejad, M., Mahmoudi, H., Ahmadi, R. and Iman-Eini, H., "A New High-Switching-Frequency Modulation Technique to Improve the DC-Link Voltage Utilization in Multilevel Converters," *IEEE Transactions on Industrial Electronics*, vol. 64, no. 3, pp. 1807-1817, March 2017.

[23] Ahn, Kang-Soon, Nam-Sup Choi, Eun-Chul Lee, and Hee-Jun Kim. "A Study on a Carrier Based PWM having Constant Common Mode Voltage and Minimized Switching Frequency in Three-level Inverter," *Journal of Electrical Engineering and Technology*, vol. 11, no. 2, pp. 393-404, 2016.

[24] Hoda Ghoreishy, Ali Yazdian Varjaniy, Shahrokh Farhangi, and Mustafa Mohamadian, "A novel pulse-

width and amplitude modulation (PWAM) control strategy for power converters," *Journal of Power Electronics*, vol. 10, no. 4, pp. 374-381, 2010.

[25] Pan, Lei, Hexu Sun, Beibei Wang, Yan Dong, and Rui Gao. "ESL-Γ-Z-Source Inverter," *Journal of Electrical Engineering and Technology*, vol. 9, no. 2, pp. 589-599, 2014.

[26] Y. Liu, B. Ge, H. Abu-Rub, F. Peng, "An effective control method for quasi-Z-source cascade multilevel inverter based grid-tie single-phase photovoltaic power system," *IEEE Trans. on Industrial Informatics*, 2013, doi: 10.1109/TII.2013.2280083

[27] Yan Zhou, Liming Liu, Hui Li, "A high-performance photovoltaic module-integrated converter (MIC) based on cascaded quasi-Z-source inverters (qZSI) using eGaN FETs," *IEEE Transactions on Power Elec-tronics*, vol. 28, no. 6, pp. 2727-2738, June 2013.

[28] R. Seyezhai and D. Umarani, "Study of Z-Source Inverter Impedance Networks using 2ω Analysis for Photovoltaic Applications," *Applied Mechanics and Materials*, vol. 852, pp. 867-874, 2016.

[29] R. Seyezhai and D. Umarani, "Total Power Control for Quasi Z-Source Inverter based Grid Tie Single Phase Photovoltaic System," *Journal of applied Sciences Research*, vol. 11, no. 14, pp. 59-66, September 2015.

[30] R. Seyezhai and D. Umarani, "Modelling and Control of Quasi Z-source Cascaded H-Bridge Multilevel Inverter for Grid Connected Photovoltaic Systems," *Energy Procedia*, vol. 90, pp. 250-259, 2016

[31] Y. Liu, H. Abu-Rub, B. Ge, F. Z. Peng, "Phase-shifted pulse-width amplitude modulation for quasi-Z-source cascade multilevel inverter based PV power system," *in Proceedings of IEEE Energy Conversion Congress & Exposition* (*ECCE*), Denver, CO, pp. 94-100, Sep. 15-19, 2013.

[32] Y. Liu, B. Ge, H. Abu-Rub, F. Peng, "An effective control method for quasi-Z-source cascade multilevel inverter based grid-tie single-phase photovoltaic power system," *IEEE Trans. on Industrial Infor-matics*, 2013, doi: 10.1109/TII.2013.2280083

[33] Aleenejad, M., Mahmoudi, H., Ahmadi, R. and Iman-Eini, H., "A New High-Switching-Frequency Modulation Technique to Improve the DC-Link Voltage Utilization in Multilevel Converters," *IEEE Transactions on Industrial Electronics*, vol. 64, no. 3, pp. 1807-1817, March 2017.

[34] Ayad, Ayman, Petros Karamanakos, and Ralph Kennel. "Direct Model Predictive Current Control Strategy of Quasi-Z-Source Inverters," *IEEE Trans-actions on Power Electronics*, vol. 32, no. 7, pp. 5786-5801, 2017.

[35] Liu, Yushan, Haitham Abu-Rub, Baoming Ge, and Fang Zheng Peng. "Phase-shifted pulse-width-amplitude modulation for quasi-Z-source cascade multilevel inverter based PV power system," *IEEE Energy Conversion Congress and Exposition* (*ECCE*), pp. 94-100, 2013.

R. Seyezhai She received obtained her B.E. (Electronics & communication Engineering) from Noorul Islam College of Engineering, Nagercoil in 1996 and her M.E in Power Electronics & Drives from Shanmugha College of Engineering, Thanjavur in 1998 and Ph.D from Anna University, Chennai, in 2010. She has been working in the teaching field for about 15 Years. She has published 140 papers in the area of Power Electronics & Drives. Her areas of interest include SiC Power Devices & Multilevel Inverters.

D. Umarani She received her B.E degree (Electrical and Electronics) in the year 2011 from Mepco Schlenk Engineering College, Sivakasi and M.E in Power Electronics and Drives from SSN College of Engineering, Chennai, in 2014. Currently she an assistant professor at SSN College of Engineer-ing, Chennai. Her areas of interest are Z-Source and Quasi Z-Source inverters, PV applications and AC Drives.